A design combining kinematic and dynamic balancing considerations with bi-material links for four-bar linkages

Ren-Chung Soong *

Kuei-Shu Hsu

Department of Mechanical and Automation Engineering

Kao Yuan University

1821 Chung-Shan Rd., Lu-Chu Hsiang

Kaohsiung 82141

Taiwan

R.O.C.

Abstract

A new design method of kinematic and dynamic integrated design for planar linkages is proposed in this paper. By properly designing the parameters of composite links that are composed of two kinds of materials, link dimensions and speed trajectory of the input link, the kinematic design requirements and expected dynamic balancing performance are satisfied. The dynamic design is by means of determining the link length proportion of occupation between the two different materials that had been selected on each movable link. The speed trajectory of the input link is designed with Bezier curves. Optimization is applied to find optimal design parameters for meeting kinematic and dynamic design requirements and constraints. Examples of four-bar linkages are given to demonstrate the feasibility of this approach.

Keywords : *Variable input speed, planar linkages, dynamic balancing design, bi-material link.*

1. Introduction

Links of a linkage, in general, are made of the same single material such as steel or alloy of aluminum. The position of mass center of each link will be at its center of geometry, if its thickness is kept the same over entire link. The dynamic balancing performance of a linkage, such as shaking force, shaking moments and driving torque, are much influenced

E-mail: soongrc@cc.kyit.edu.tw

Journal of Information & Optimization Sciences

Vol. ( ), No. , pp. 1–24

by its inertial properties of mass center, for example, the position, velocity, and magnitude of mass center. Therefore, they would be regulated, if it is possible to change the inertial properties of mass center of each link in a linkage.

The concept of bi-material link is that the link is composed of two parts with different materials connected by any possible means. So, the inertial properties of mass center of a linkage could be adjusted by determining the proportion of length between two parts.

Since the dynamic balancing performance of a linkage are not only affected by inertial properties but also velocity and acceleration of mass center of each link. Therefore, it is possible to gain the better results, if we could tune the speed trajectory of input link.

Furthermore, the inertial properties and kinematic characteristics of mass center of each link of a linkage will vary with the change of link length. For this reason, it is a feasible way to get a linkage, which satisfies kinematic design requirements and constraints and posses the expected dynamic balancing performance, if we combine kinematic synthesis and dynamic design in the same design stage.

Possessing the good dynamic balancing performance is essentially demanded for high-speed applications to linkages. For examples, minimum shaking force, shaking moments and driving torque even for complete force balance. These dynamic balancing quantities would cause the inaccuracies, noises, vibrations and fatigues of the desired mechanisms. Unfortunately, they usually conflict each other, so the trade-off of dynamic balancing may be a reasonable choice.

Kinematic synthesis and dynamic design are both essential steps in the development of mechanisms and are usually treated as separate stages in the design process, and traditionally, the input speed of the driving link is assumed constant.

Our purpose here is to develop a method, which combines kinematic synthesis, dynamic design, and input speed trajectory design, to reach the trade-off of dynamic balance and to satisfy the kinematic requirements and constraints simultaneously for four-bar linkages by using bi-material links.

The researches which are related to the combination of kinematic synthesis and dynamic design are not many in the literature. Conte *et al.* [1] synthesized the crank-rocker path generating mechanisms with prescribed timing by optimization based on minimizing shaking force, driving torque, and bearing reactions, respectively. Yan and Soong [2] have

been devoted to study on the subject of kinematic and dynamic integrated design for four-bar linkages with variable input speed trajectory for several years.

In general, there are two major different approaches of the trade-off of dynamic balancing design for planar linkages. One is by positioning a counterweight on each movable link [12, 13]. The other one is by mass redistribution of each movable link [11, 14]. Using the concept of bi-material links for dynamic balancing design might be the first proposed.

As a result of the progress of the servo control technology, the variable input speed mechanisms were paid much attention on machine design in pass decade. Kochev [3] applied a prescribed input speed fluctuation to the complete force balanced linkages for balancing the shaking moment. Yan and associates [4-6] contributed the objectives of eliminating the discontinuity in motion characteristics and lowering peak values of the follower acceleration in cam-follower systems by servo control. Yan and Chen [7] further designed a general input speed trajectory for slider-crank mechanisms that lead to arbitrarily desired output motion.

Methods of balancing shaking force and shaking moment in high-speed machinery are well-developed and documented [3, 8-15]. Most of the balancing methods dealt directly with the shaking force involved, or the shaking moment fluctuations [8-9]. Some articles included bearing reaction magnitudes [11, 14] and input torque fluctuations [10-13]. However, very few methods allow a trade-off among variations and the magnitudes of the shaking force, shaking moment, bearing reaction and the input torque [11, 14].

2. Bi-material link

The bi-material link is composed of two different materials as shown in Figure 1, named as the standard bi-material link.

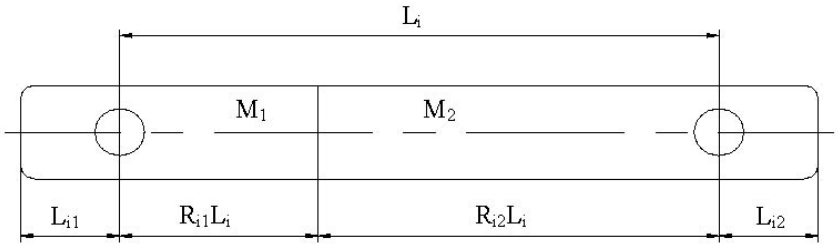

Figure 1
The bi-material link

where M_1 and M_2 represent parts made of the two kinds of materials, respectively, L_i is the ith link length in the linkage, R_{i1} and R_{i2} are the percentage of occupation of the ith link length belong to M_1 and M_2, respectively, and $R_{i1} + R_{i2} = 1$, L_{i1} and L_{i2} are the parts of overhang out of two pivots on the ith link belong to M_1 and M_2, respectively.

There are two ways of material distribution on each movable link. For four-bar linkages, there are eight possible ways for material distribution as shown in Figure 2.

In order to obtain the better dynamic balancing performance, we can reach the goal by determining the way of material distribution such as the one of the ways as shown in Figure 2 and properly designing dynamic balancing parameters such as R_{i1}, R_{i2}, L_{i1} and L_{i2} to have corresponding inertial properties of the center of mass of each movable link.

3. Input speed trajectory

We assume the input link of the four-bar linkage is a crank. The position trajectory of the crank is defined by an nth order Bezier curve $\phi(t)$ with parameter t as follows:

$$\phi(t) = \sum_{i=0}^{n} \theta_i \cdot B_{i,n}(t)\,, \tag{1}$$

where

$$B_{i,n}(t) = \frac{n!}{i! \cdot (n-i)!} \cdot t^i \cdot (1-t)^{n-i}\,, \quad t \in [0,1] \tag{2}$$

in which $\phi(t)$ is a Bezier curve that represents the angular displacement of the input link defined by control points θ_i. Parameter t is regarded as the normalized time from 0 to 1. Since the Bezier curve is nth order differentiable, this guarantees smoothness of the entire motion. Hence, the angular velocity $\omega(t)$ and acceleration $\alpha(t)$ of the input link can be derived by continuously differentiating Eqs. (1) and (2) with respect to the time as follows:

$$\omega(t) = \frac{d\phi(t)}{dt} = \sum_{i=0}^{n} \theta_i \cdot \frac{dB_{i,n}(t)}{dt}\,, \tag{3}$$

$$\alpha(t) = \frac{d^2\phi(t)}{dt^2} = \sum_{i=0}^{n} \theta_i \cdot \frac{d^2B_{i,n}((t)}{dt^2}\,, \tag{4}$$

where

$$\begin{aligned} \frac{dB_{i,n}(t)}{dt} &= \frac{n!}{(i-1)! \cdot (n-i)!} \cdot t^{i-1} \cdot (1-t)^{n-i} \\ &\quad - \frac{n!}{i! \cdot (n-i-1)!} \cdot t^i \cdot (1-t)^{n-i-1}\,, \end{aligned} \tag{5}$$

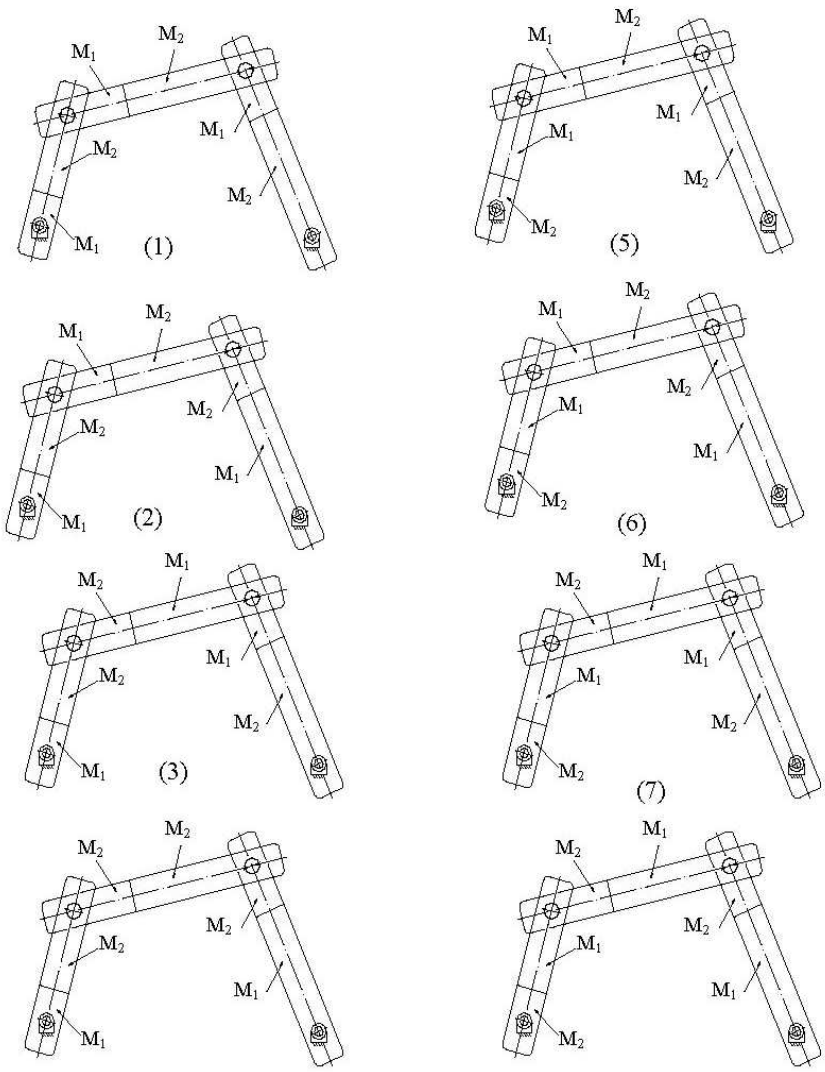

Figure 2
The possible ways of material distribution for four-bar linkages

$$\frac{d^2 B_{i,n}(t)}{dt^2} = \frac{n!}{(i-2)! \cdot (n-i)!} \cdot t^{i-2} \cdot (1-t)^{n-i} - \frac{n!}{(i-1)! \cdot (n-i-1)!} \cdot t^{i-1} \cdot (1-t)^{n-i-1}$$

$$- \frac{n!}{(i-1)! \cdot (n-i-1)!} \cdot t^{i-1} \cdot (1-t)^{n-i-1}$$
$$+ \frac{n!}{i! \cdot (n-i-2)!} \cdot t^{1} \cdot (1-t)^{n-i-2} . \quad (6)$$

After doing the kinematic analysis of the four-bar linkage by vector loop approach (16), all the kinematic magnitudes (positions, velocities and accelerations) of each moving links and their center of mass can be obtained as function of the crank motion.

4. Dynamic equations

The general analytical model and inertial properties of each moving link is represented, as show in Figure 3. Link elasticity and friction in the joints are neglected. The principle of virtual work and Newtonian dynamic analytical method are used to derive dynamic equations.

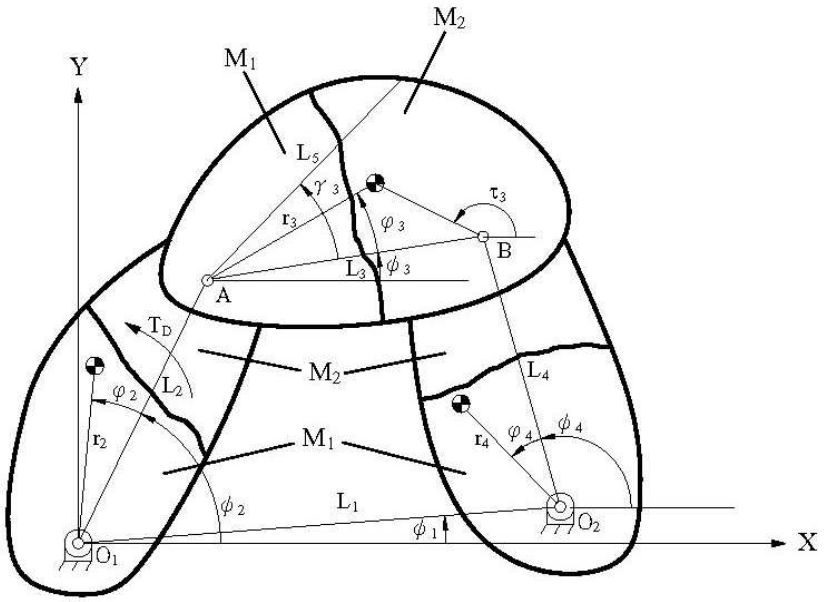

Figure 3
The dynamic analytical model for four-bar linkages

If the movable links in the general analytical model are all replaced by standard link as shown in Figure 1, by applying the principle of virtual work to the system shown in Figure 3, the driving torque T_D is obtained

as follow:

$$T_D\left(L_1,\ldots,L_4,\phi_1,\theta_0,\ldots,\theta_n,R_{i1},L_{i1},L_{i2}\right)=\sum_{i=2}^{4}\frac{k_i}{\omega_2}\,, \tag{7}$$

where

$$k_i = m_i\mathbf{a}_i\mathbf{v}_i + I_i\alpha_i\omega_i - T_{ei}\omega_i \tag{8}$$

in which m_i is the mass of the ith link, ω_i and α_i are, respectively, the angular velocity and angular acceleration of the ith link, T_{ei} and $\mathbf{F}_{ei}$ are, respectively, the working torque and force applied on the ith link, $\mathbf{v}_{ei}$ is the linear velocity vector of point of working forces applied on the ith link, I_i is the moment of inertial of ith link about its center of gravity, $\mathbf{v}_i$ and $\mathbf{a}_i$ are, respectively, the velocity and acceleration vector of center of gravity of the ith link, ϕ_1 is the angles measured from X axis to the center line between two fixed pivots.

Now, T_D divided by $m_{2R}L_{2R}^2\omega_{2av}^2$, we have the normalized driving torque T_D° as follows:

$$T_D^\circ = \sum_{i=2}^{4}\frac{k_i}{m_{2R}L_{2R}^2\omega_{2av}^2} \tag{9}$$

in which m_{2R}, L_{2R} and ω_{2av} are the mass, the link length and the average angular velocity of the input link of the reference linkage respectively.

Furthermore, by applying the virtual work principle to the free-body diagrams shown in Figures 4(a)-(c), we obtain close-form expressions for computing the reaction forces of coupler joints A and B as follows:

$$F_{23x} = \frac{(Rv_{Bx}+Sv_{By}-P)v_{Ay}-Qv_{By}}{V}\,, \tag{10}$$

$$F_{23y} = \frac{(P-Rv_{Bx}-Sv_{By})v_{Ax}+Qv_{Bx}}{V}\,, \tag{11}$$

$$F_{43x} = \frac{(P-Sv_{By})v_{Ay}-(Rv_{Ax}-Q)v_{By}}{V}\,, \tag{12}$$

$$F_{43y} = \frac{(Rv_{Bx}-P)v_{Ay}+(Sv_{Ay}-Q)v_{Bx}}{V}\,, \tag{13}$$

where

$$P = \sum_{i=2}^{3}k_i - T_D\omega_2\,, \tag{14}$$

$$Q = \sum_{i=3}^{4}k_i\,, \tag{15}$$

$$R = m_3a_{3x}\,, \tag{16}$$

$$S = m_3 a_{3y}\,, \tag{17}$$

$$V = v_{Bx}v_{Ay} - v_{By}v_{Ax}\,. \tag{18}$$

in which F_{eix} and F_{eiy} are, respectively, x and y components of the working forces applied on the ith link, F_{ijx} and F_{ijy} are, respectively, x and y components of forces exerted on the jth link by the ith link, v_{Ax} and v_{Ay} are, respectively, x and y components of the velocity of point A on link 3, v_{Bx} and v_{By} are, respectively, x and y components of the velocity of point B on link 3, a_{ix} and a_{iy} are, respectively, x and y components of the acceleration of the center of gravity of the ith link.

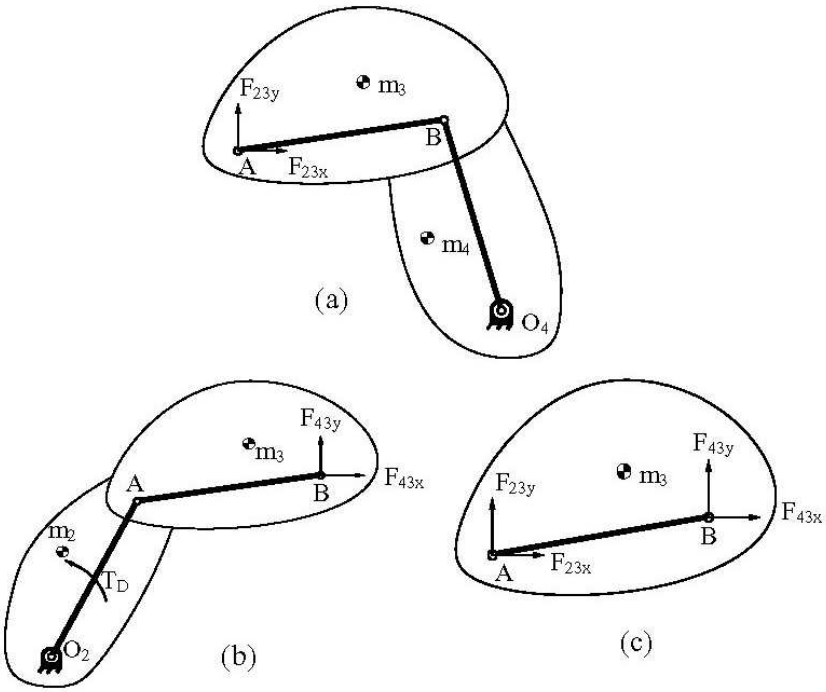

Figure 4

The free-body diagrams of four-bar linkages

By solving the equilibrium equations (10)-(13), we obtain all unknown reaction forces F_{12} and F_{14} of joints as follows:

$$F_{12x} = F_{23x} + m_2 a_{2x}\,, \tag{19}$$

$$F_{12y} = F_{23y} + m_2 a_{2y}\,, \tag{20}$$

$$F_{14x} = F_{43x} + m_4 a_{4x}\,, \tag{21}$$

$$F_{14y} = F_{43y} + m_4 a_{4y}\,. \tag{22}$$

Once all joint forces are determined, the shaking force and shaking moments with respect to fixed pivot o_i can be formulated as follows:

$$F_{sh} = (F_{21x} + F_{41x})\mathbf{i} + (F_{21y} + F_{41y})\mathbf{j} \tag{23}$$

in which β_i is the angles measured counterclockwise from X axis to the point of working forces applied on the ith link, s_i is the distance to the fixed or moving pivot as measured from the applied point of working forces on the ith link.

Then, F_{sh} and $M_{\underset{o_i}{sh}}$ divided by $m_{2R}L_{2R}\omega_{2av}^2$ and $m_{2R}L_{2R}^2\omega_{2av}^2$, respectively, we have the normalized shaking force and shaking moments with respect to fixed pivot o_i as follows:

$$F_{sh}^{\circ} = \frac{F_{sh}}{m_{2R}L_{2R}\omega_{2av}^2}\,. \tag{24}$$

5. Optimization

In order to reach a trade-off of dynamic balancing of four-bar linkages that fulfill the kinematic design requirements, first, the materials composed of composite links are selected, then, the undetermined control points $(\theta_0, \theta_1, \ldots, \theta_{n-1}, \theta_n)$, link dimensions $(L_i,\ i = 1 \sim 4, \phi_i)$ and dynamic balancing parameters $(R_{i1}, L_{i1}, L_{i2},\ i = 2 \sim 4)$ are determined by optimization procedure. It is clear that θ_0 and θ_n are the boundary conditions for the crank displacement in a cycle. Therefore, $\theta_0 = 0$ and $\theta_n = 360$ must be specified.

The objective function and constraint equations are formulated as follows:

Minimizing

$$\begin{aligned} &f(L_1, \ldots, L_4, \phi_1, \theta_1, \ldots, \theta_{n-1}, R_{i1}, L_{i1}, L_{i2}) \\ &\quad = \sum_{\delta=1}^{n_s} w_{k\delta} obj_{k\delta} + w_{d\delta} obj_{d\delta} \end{aligned} \tag{25}$$

Subject to equality constraints

$$c_j(L_1, \ldots, L_4, \phi_1, \theta_1, \ldots, \theta_{n-1}, R_{i1}, L_{i1}, L_{i2}) = 0\,,\ j = 1, \ldots, n_c \tag{26}$$

and inequality constraints

$$g_j(L_1, \ldots, L_4, \phi_1, \theta_1, \ldots, \theta_{n-1}, R_{i1}, L_{i1}, L_{i2}) < 0\,,\ j = 1, \ldots, n_g\,, \tag{27}$$

where $obj_{k\delta}$ and $obj_{d\delta}$ are kinematic and dynamic objective function respectively, $w_{k\delta}$ and $w_{d\delta}$ are kinematic and dynamic weighting factors, respectively, n_s denotes the number of kinematic and dynamic objec-

tive function, n_c and n_g denote the number of equality and inequality constraints equations, respectively. Note that the equality and inequality constraints are defined to meet the desired characteristics of output motion and dynamic balancing performance.

Up to here, all information for optimization has been derived. Any optimization methods can be used to determine the design variables. An optimization program namely MOST [17] that is developed for solving multi-objective optimization problems with mixed continuous and discrete design variables is used to solve design variables in the present approach.

6. Examples and discussions

Here we demonstrate the feasibility of this proposed approach by three examples including motion generation, function generation and path generation with prescribing time.

In following examples, the objective is focused on reaching the trade-off of dynamic balancing performance under the conditions that meet the kinematic requirements and constraints. Therefore, the objective function is defined as follow:

$$f(L_1,\ldots,L_4,\phi_1,\theta_1,\ldots,\theta_9,R_{i1},L_{i1},L_{i2}) = \frac{1}{2\pi}\int_0^{2\pi}\left[w_{d1}\sqrt{F_{21}^{\circ 2}+F_{41}^{\circ 2}}+w_{d2}\sqrt{T_D^{\circ 2}}\right]d\phi_2\,. \tag{28}$$

But the equality and inequality constraints equations are different depending on kinematic design requirements and constraints for different design cases.

A 10th order Bezier curve (with 11 control points) is used to represent the trajectory of the crank displacement, the weighting factors w_{d1} and w_{d2} are both set to be 0.5 for the trade-off of dynamic balancing, and the optimization task is to determine the control points $(\theta_1,\ldots,\theta_9)$ and balancing parameters $(R_{i1},L_{i1},L_{i2},\ i=2\sim 4)$ and link dimensions $(L_i,\ i=1\sim 4,\phi_i)$, and to compare the dynamic balancing performance with the reference linkage shown in Figure 5 has its link dimensions and inertial properties given in Table 1 and running at an average crank speed of 60 rpm in following examples.

There are three design cases in each example. The ratio of specific gravity of two different materials composed of composite links and the limit of the overhang on each composite link are shown in Table 2.

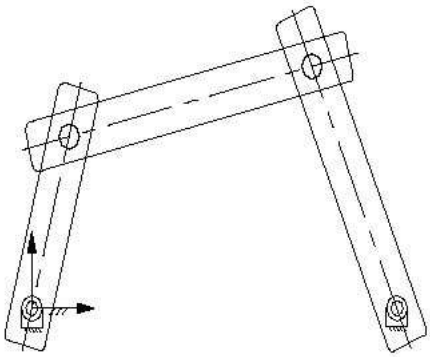

Figure 5
The reference linkage

Table 1
Link dimensions of the reference linkage

Link number	Length of link (m)	Width of link (m)	Thickness of link (m)
1	0.0762	0.0127	0.005
2	0.0254	0.0127	0.005
3	0.0508	0.0127	0.005
4	0.0762	0.0127	0.005

Table 2
Ratio of specific gravity and Limit of the overhang (m)

Design case	Ratio of specific gravity	Upper limit of the overhang (m)	Lower limit of the overhang (m)
1	$M_1/M_2 = 1/2$	0.03	0.005
2	$M_1/M_2 = 1/2$	0.05	0.005
3	$M_1/M_2 = 1/5$	0.03	0.005

Example 1. Designing the input speed trajectory, balancing parameters of links and link dimensions of a desired linkage in which the couple point passes three precision points as B_1(0.0381m, 0.0660m), B_2(0.0248m, 0.0563m) and B_3(0.0159m, 0.0466m) with prescribing time at $t_1 = 0.11$, $t_2 = 0.31$ and $t_3 = 0.39$ for trade-off of dynamic balancing respectively, and the cross section of links are kept the same with the reference linkage.

The objective function and constraint equations become as follows:

Minimizing equation (35)

Subject to

$$c_1(\theta_1,\ldots,\theta_9) = \omega_2(0) - \omega_2(1) = 0\,,$$
$$c_2(\theta_1,\ldots,\theta_9) = \alpha_2(0) - \alpha_2(1) = 0\,,$$
$$c_3(L_1,\ldots,L_4,\phi_1,\theta_1,\ldots,\theta_9) = \phi_2(0.11) = B_{1x} - 0.038 = 0\,,$$
$$c_4(L_1,\ldots,L_4,\phi_1,\theta_1,\ldots,\theta_9) = \phi_2(0.11) = B_{1y} - 0.066 = 0\,,$$
$$c_5(L_1,\ldots,L_4,\phi_1,\theta_1,\ldots,\theta_9) = \phi_2(0.31) = B_{2x} - 0.0248 = 0\,,$$
$$c_6(L_1,\ldots,L_4,\phi_1,\theta_1,\ldots,\theta_9) = \phi_2(0.31) = B_{2y} - 0.0563 = 0\,,$$
$$c_7(L_1,\ldots,L_4,\phi_1,\theta_1,\ldots,\theta_9) = \phi_2(0.39) = B_{3x} - 0.0159 = 0\,,$$
$$c_8(L_1,\ldots,L_4,\phi_1,\theta_1,\ldots,\theta_9) = \phi_2(0.39) = B_{3y} - 0.0466 = 0\,,$$
$$c_9(L_1,\ldots,L_4) = L_{\min} - L_2 = 0\,,$$
$$g_{k+1}(L_1,\ldots,L_4) = (L_{\min} + L_{\max}) - (L_p + L_q) < 0\,.$$

The first two constrained equations are in order to have continuous angular velocity and acceleration of the input link in two consecutive cycles and the third to the eighth are for fulfilling the kinematic design requirements, and the last two are the Grashof criteria for a crank-rocker mechanism. The optimal control points, link dimensions and balancing parameters are respectively shown in Tables 3 and 4, and the comparisons of rms dynamic quantities are shown in Table 5. The corresponding input and output motion characteristics and the comparisons of dynamic balancing performance are shown in Figures 6 and 7, respectively.

Table 3

Control points of trajectory of driving link for Example 1

Design case	$\theta_1(^\circ)$	$\theta_2(^\circ)$	$\theta_3(^\circ)$	$\theta_4(^\circ)$	$\theta_5(^\circ)$	$\theta_6(^\circ)$	$\theta_7(^\circ)$	$\theta_8(^\circ)$	$\theta_9(^\circ)$
1	22.60	48.69	115.59	159.93	188.75	240.45	300.66	318.29	337.39
2	31.58	64.71	111.33	144.17	180.96	219.78	257.92	298.37	328.41
3	30.00	62.14	112.22	148.69	183.54	221.07	259.97	302.14	329.99

Table 4

Link dimensions and balancing parameters for Example 1

Design case	L_1 (cm)	L_2 (cm)	L_3 (cm)	L_4 (cm)	ϕ_1 $(^\circ)$	R_{21}	R_{31}	R_{41}	L_{21} (cm)	L_{22} (cm)	L_{31} (cm)	L_{32} (cm)	L_{41} (cm)	L_{42} (cm)
1	7.96	1.99	3.04	7.62	−22.9	1	1	1	3	0.5	0.5	0.5	0.5	1.45
2	8.50	2.36	4.41	7.62	−10.98	1	1	1	5	0.5	3.2	0.5	0.5	1.87
3	8.32	2.30	4.11	7.62	−13.18	1	1	1	3	0.5	2.81	0.5	0.5	1.44

Table 5

Comparison of the dynamic quantities between Example 1

Design case	r.m.s shaking force	r.m.s bearing reaction force to fixed pivot o_2	r.m.s bearing reaction force to fixed pivot o_4	r.m.s driving torque
Reference linkage	4.1691	4.1053	1.6786	1.7443
1	1.5698(62%)	1.4262(65%)	0.7648(54%)	0.7894(55%)
2	1.3446(68%)	1.1403(72%)	0.9528(43%)	0.5930(66%)
3	1.276(69%)	1.1566(71%)	0.8586(49%)	0.6447(63%)

The value in parentheses denotes percent improvement over the corresponding rms value of the linkage number 1

Example 2. Designing the input speed trajectory, balancing parameters of links and link dimensions of a desired linkage in which the moving pivot B passes three precision points as B_1(0.0381m, 0.0660m), B_2(0.0248m, 0.0563m) and B_3(0.0159m, 0.0466m) and the coupler turns -11.8° and -13.2° respectively, while the point B moving from B_1 to B_2 and B_1 to B_3 for trade-off of dynamic balancing respectively, and the cross section of links are kept the same with the reference linkage.

The objective function is the same with Example 1, and the constraint equations become as follows:

Minimizing equation (28)

Subject to

$$
\begin{aligned}
&c_1(\theta_1,\ldots,\theta_9) = \omega_2(0) - \omega_2(1) = 0\,,\\
&c_2(\theta_1,\ldots,\theta_9) = \alpha_2(0) - \alpha_2(1) = 0\,,\\
&c_3(L_1,\ldots,L_4,\phi_1,\theta_1,\ldots,\theta_9) = B_{1x} - 0.038 = 0\,,\\
&c_4(L_1,\ldots,L_4,\phi_1,\theta_1,\ldots,\theta_9) = B_{1y} - 0.066 = 0\,,\\
&c_5(L_1,\ldots,L_4,\phi_1,\theta_1,\ldots,\theta_9) = B_{2x} - 0.0248 = 0\,,\\
&c_6(L_1,\ldots,L_4,\phi_1,\theta_1,\ldots,\theta_9) = B_{2y} - 0.0563 = 0\,,\\
&c_7(L_1,\ldots,L_4,\phi_1,\theta_1,\ldots,\theta_9) = B_{3x} - 0.0159 = 0\,,\\
&c_8(L_1,\ldots,L_4,\phi_1,\theta_1,\ldots,\theta_9) = B_{3y} - 0.0466 = 0\,,\\
&c_9(L_1,\ldots,L_4,\phi_1,\theta_1,\ldots,\theta_9) = \phi_{32} - \phi_{31} + 11.8^\circ = 0\,,\\
&c_{10}(L_1,\ldots,L_4,\phi_1,\theta_1,\ldots,\theta_9) = \phi_{33} - \phi'_{31} + 13.2^\circ = 0\,,\\
&c_9(L_1,\ldots,L_4) = L_{\min} - L_2 = 0\,,\\
&g_{k+1}(L_1,\ldots,L_4) = (L_{\min} + L_{\max}) - (L_p + L_q) < 0\,.
\end{aligned}
$$

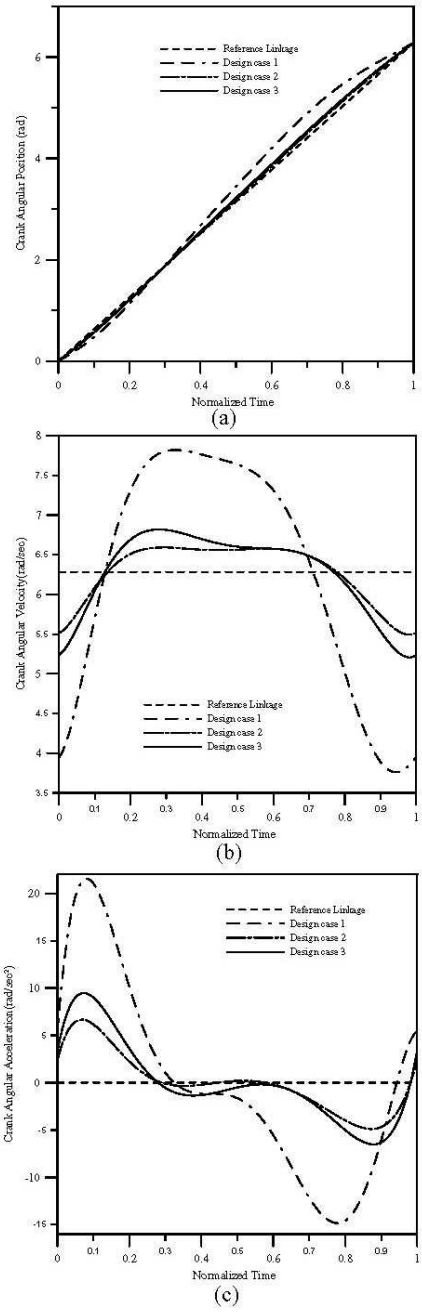

Figure 6

Input motion characteristics – Example 1

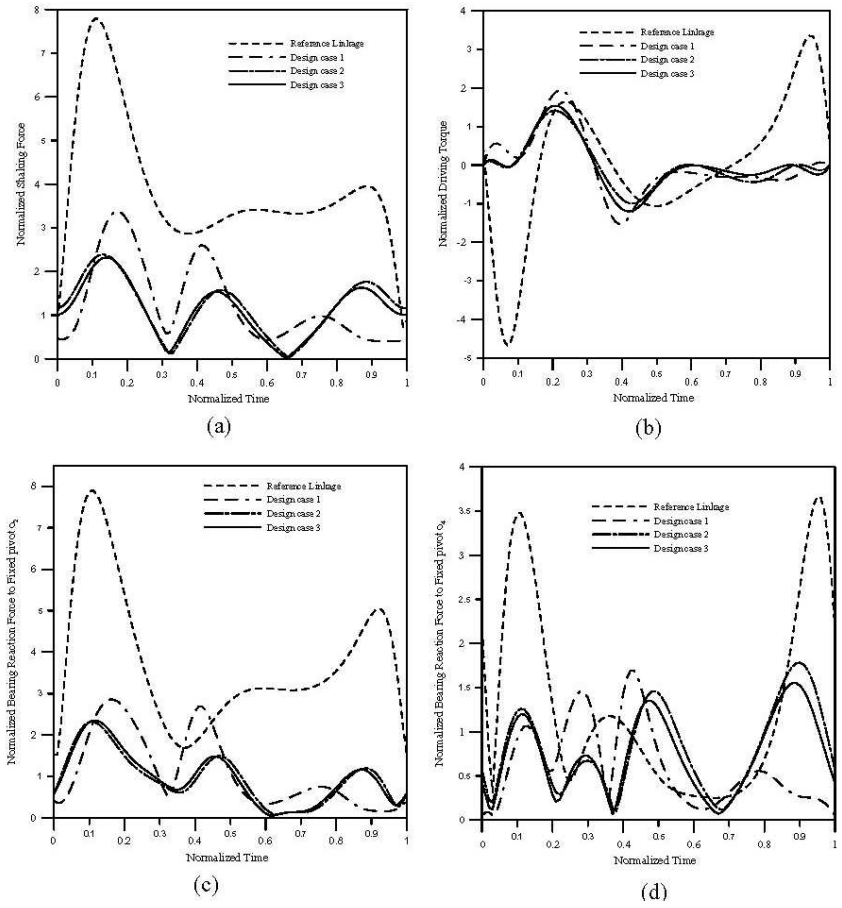

Figure 7

Dynamic balancing performance – Example 1

The first two constrained equations have the same purpose as Example 1, the third to the tenth are for fulfilling the kinematic design requirements, and the last two are the Grashof criteria for a crank-rocker mechanism. The optimal control points, link dimensions and balancing parameters are respectively shown in Tables 6 and 7, and the comparisons of rms dynamic quantities are shown in Table 8. The corresponding input motion characteristics and the comparisons of dynamic balancing performance are shown in Figures 8 and 9, respectively.

Table 6

Control points of trajectory of driving link for Example 2

Design case	$\theta_1(^\circ)$	$\theta_2(^\circ)$	$\theta_3(^\circ)$	$\theta_4(^\circ)$	$\theta_5(^\circ)$	$\theta_6(^\circ)$	$\theta_7(^\circ)$	$\theta_8(^\circ)$	$\theta_9(^\circ)$
1	41.55	95.82	112.44	127.28	165.53	219.00	265.22	289.64	318.45
2	36.33	74.49	113.42	135.78	176.83	219.25	252.94	289.14	323.66
3	36.97	78.87	115.44	132.12	170.70	218.12	255.74	290.98	323.03

Table 7

Link dimensions and balancing parameters for Example 2

Design case	L_1 (cm)	L_2 (cm)	L_3 (cm)	L_4 (cm)	ϕ_1 $(^\circ)$	R_{21}	R_{31}	R_{41}	L_{21} (cm)	L_{22} (cm)	L_{31} (cm)	L_{32} (cm)	L_{41} (cm)	L_{42} (cm)
1	10.89	1.64	5.66	7.62	-20.5	1	1	1	3	0.5	0.5	0.5	0.5	1.16
2	11.00	1.77	6.32	7.62	-14.0	1	1	1	5	0.5	4.69	0.5	0.5	1.79
3	10.22	1.85	5.46	7.62	-16.9	1	1	1	2.98	1.35	3	0.5	0.5	1.31

Table 8

Comparison of the dynamic quantities between Example 2

Design case	r.m.s shaking force	r.m.s bearing reaction force to fixed pivot o_2	r.m.s bearing reaction force to fixed pivot o_4	r.m.s driving torque
Reference linkage	4.1691	4.1053	1.6786	1.7443
1	1.4347 (66%)	1.4290 (65%)	0.7632 (55%)	0.1794 (89%)
2	0.9768 (77%)	0.8112 (80%)	0.9768 (42%)	0.1191 (93%)
3	1.034 (75%)	0.9905 (76%)	0.6595 (61%)	0.1394 (92%)

The value in parentheses denotes percent improvement over the corresponding rms value of the reference linkage

Example 3. Designing the input speed function, balancing parameters of links and the link dimensions of a desired linkage in which the moving pivot B passes three precision points as B_1(0.0381m, 0.0660m), B_2(0.0248m, 0.0563m) and B_3(0.0159m, 0.0466m) and the input link and output link turn 61° and 91° and 12.3° and 22.2° respectively, while the point B moving from B_1 to B_2 and B_1 to B_3 for trade-off of dynamic balancing respectively, and the cross section of links are kept the same with the reference linkage.

The objective function is the same with the former two examples, and the constraint equations become as follows:

Minimizing equation (35)

Subject to

$$
\begin{aligned}
&c_1(\theta_1,\ldots,\theta_9) = \omega_2(0) - \omega_2(1) = 0\,,\\
&c_2(\theta_1,\ldots,\theta_9) = \alpha_2(0) - \alpha_2(1) = 0\,,\\
&c_3(L_1,\ldots,L_4,\phi_1,\theta_1,\ldots,\theta_9) = B_{1x} - 0.038 = 0\,,\\
&c_4(L_1,\ldots,L_4,\phi_1,\theta_1,\ldots,\theta_9) = B_{1y} - 0.066 = 0\,,\\
&c_5(L_1,\ldots,L_4,\phi_1,\theta_1,\ldots,\theta_9) = B_{2x} - 0.0248 = 0\,,\\
&c_6(L_1,\ldots,L_4,\phi_1,\theta_1,\ldots,\theta_9) = B_{2y} - 0.0563 = 0\,,\\
&c_7(L_1,\ldots,L_4,\phi_1,\theta_1,\ldots,\theta_9) = B_{3x} - 0.0159 = 0\,,\\
&c_8(L_1,\ldots,L_4,\phi_1,\theta_1,\ldots,\theta_9) = B_{3y} - 0.0466 = 0\,,\\
&c_9(L_1,\ldots,L_4,\phi_1,\theta_1,\ldots,\theta_9) = \phi_{22} - \phi_{21} - 61^\circ = 0\,,\\
&c_9(L_1,\ldots,L_4,\phi_1,\theta_1,\ldots,\theta_9) = \phi_{23} - \phi_{21} - 91^\circ = 0\,,\\
&c_9(L_1,\ldots,L_4,\phi_1,\theta_1,\ldots,\theta_9) = \phi_{42} - \phi_{41} - 12.3^\circ = 0\,,\\
&c_9(L_1,\ldots,L_4,\phi_1,\theta_1,\ldots,\theta_9) = \phi_{43} - \phi_{41} - 22.2^\circ = 0\,,\\
&c_9(L_1,\ldots,L_4) = L_{\min} - L_2 = 0\,,\\
&g_{k+1}(L_1,\ldots,L_4) = (L_{\min} + L_{\max}) - (L_p + L_q) < 0\,.
\end{aligned}
$$

The first two constrained equations have the same purpose as Example 1, the third to the twelfth are for fulfilling the kinematic design requirements, and the last two are the Grashof criteria for a crank-rocker mechanism.

The optimal control points, link dimensions and balancing parameters are respectively shown in Tables 9 and 10, and the comparison of rms dynamic quantities are shown in Table 11. The corresponding input and output motion characteristics and the comparison of dynamic balancing performance are shown in Figures 10 and 11, respectively.

The optimal way of material distribution that is the 8th way as shown in Figure 2 is got from the design results in these examples.

We obtain the substantial improvement to each dynamic quantity not only in magnitudes but variations and satisfy kinematic design requirements and constraints simultaneously according to the design results as shown in Table 5, 8 and 11 and Figures 7, 9 and 11, respectively. Because the dynamic balancing performance of a desired linkage is dominated by inertial properties and kinematic characteristics of the center of gravity

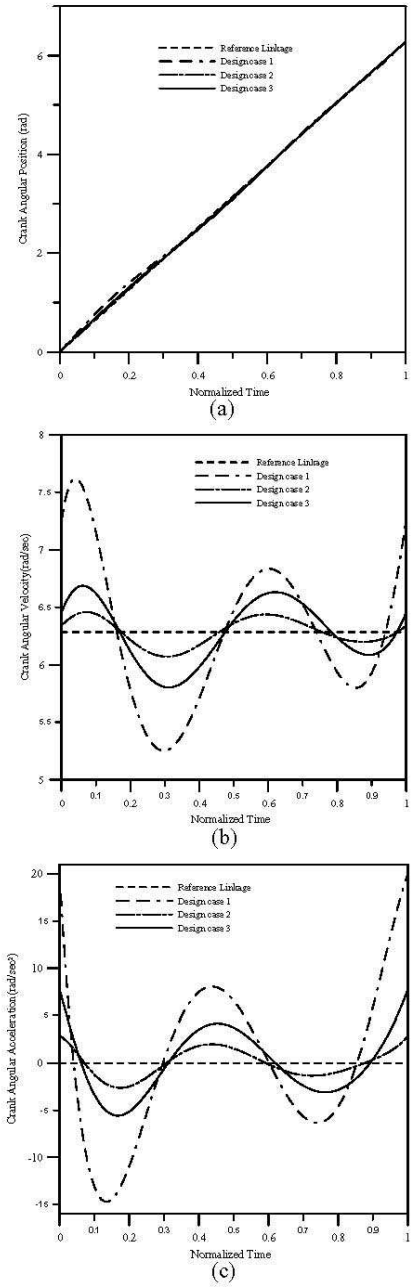

Figure 8

Input motion characteristics – Example 2

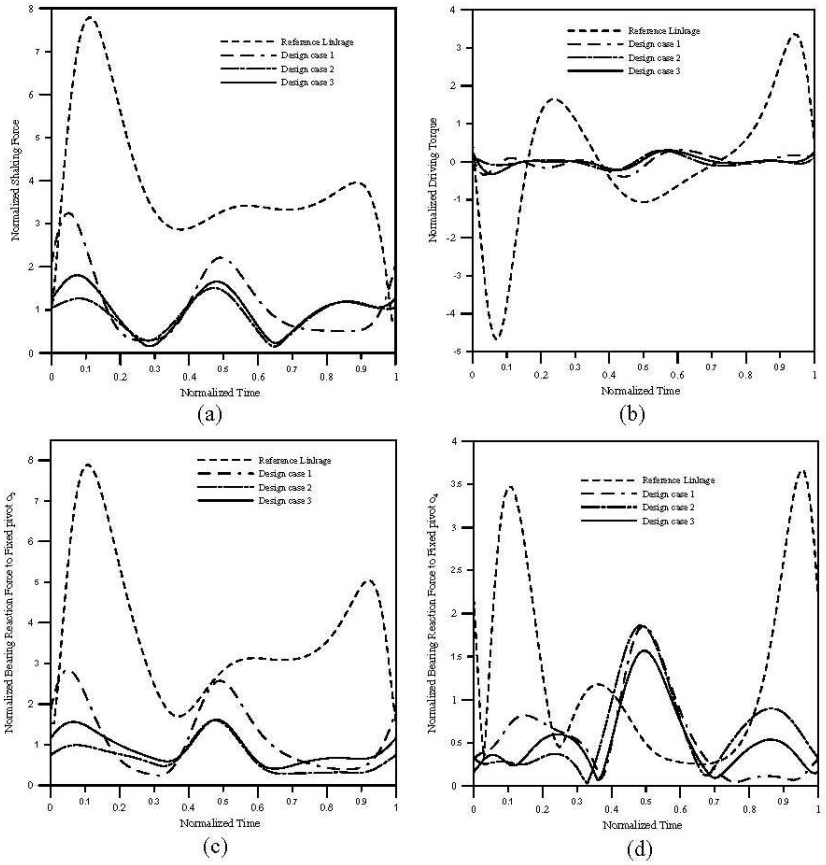

Figure 9

Dynamic balancing performance – Example 2

Table 9

Control points of trajectory of driving link for Example 3

Design case	$\theta_1(^\circ)$	$\theta_2(^\circ)$	$\theta_3(^\circ)$	$\theta_4(^\circ)$	$\theta_5(^\circ)$	$\theta_6(^\circ)$	$\theta_7(^\circ)$	$\theta_8(^\circ)$	$\theta_9(^\circ)$
1	34.43	82.29	130.54	118.52	143.23	202.16	254.66	304.56	325.56
2	34.32	70.98	122.60	127.28	168.62	219.24	249.37	293.69	325.67
3	34.99	75.43	121.09	128.15	166.22	214.79	250.08	295.43	325.00

Table 10

Link dimensions and balancing parameters for Example 3

Design case	L_1 (cm)	L_2 (cm)	L_3 (cm)	L_4 (cm)	ϕ_1 ($^\circ$)	R_{21}	R_{31}	R_{41}	L_{21} (cm)	L_{22} (cm)	L_{31} (cm)	L_{32} (cm)	L_{41} (cm)	L_{42} (cm)
1	8.46	2.04	3.21	7.62	-22.1	1	1	1	3	0.5	0.5	0.5	0.5	1.38
2	9.04	2.28	4.63	7.62	-11.6	1	1	1	5	0.5	3.20	0.5	0.5	1.99
3	8.99	2.23	4.36	7.62	-13.9	1	1	1	3	0.5	2.92	0.5	0.5	1.41

Table 11

Comparison of the dynamic quantities between Example 3

Design case	r.m.s shaking force	r.m.s bearing reaction force to fixed pivot o_2	r.m.s bearing reaction force to fixed pivot o_4	r.m.s driving torque
Reference linkage	4.1691	4.1053	1.6786	1.7443
1	1.5914 (62%)	1.5522 (62%)	0.9548 (43%)	0.3104 (82%)
2	1.3111 (68%)	1.0892 (73%)	0.9171 (45%)	0.2004 (89%)
3	1.2798 (69%)	1.1496 (72%)	0.9183 (45%)	0.2611 (85%)

The value in parentheses denotes percent improvement over the corresponding rms value of the reference linkage

of each movable link such as mass, inertial moment, position, velocity and acceleration, and they are all the function of the link dimensions, furthermore, the kinematic terms are also controlled by the kinematic characteristics of input link. That is why we integrate kinematic synthesis, dynamic balancing design and design of input speed trajectory into one design step.

7. Conclusions

A new general design approach that combines kinematic synthesis, dynamic balancing and input speed trajectory design in one design stage is proved to be feasible for planar linkages. According to the results of examples as shown in Table 3-11 and Figure 6-11, the following conclusions can be made:

1. The optimal material distribution on each moving link is shown in Figure 2(8) for all examples.
2. The lower ratio of specific gravity of two materials composed of each movable link is selected, the better trade-off dynamic balancing performance is reached.
3. The longer upper limit of overhang on two ends of each movable link is set, the better trade-off of dynamic balancing performance is reached.
4. Each dynamic quantity is minimized not only in magnitudes but fluctuations as well.

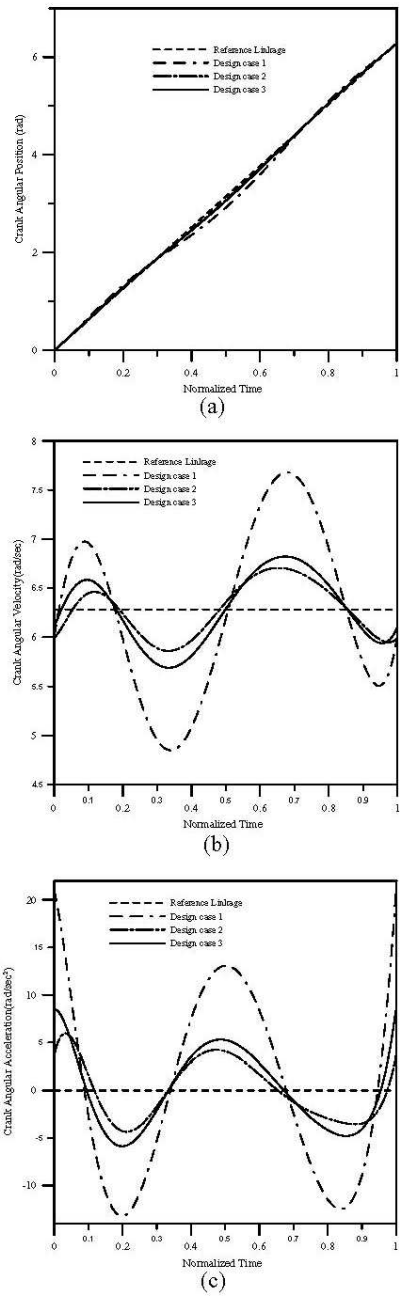

Figure 10

Input motion characteristics – Example 3

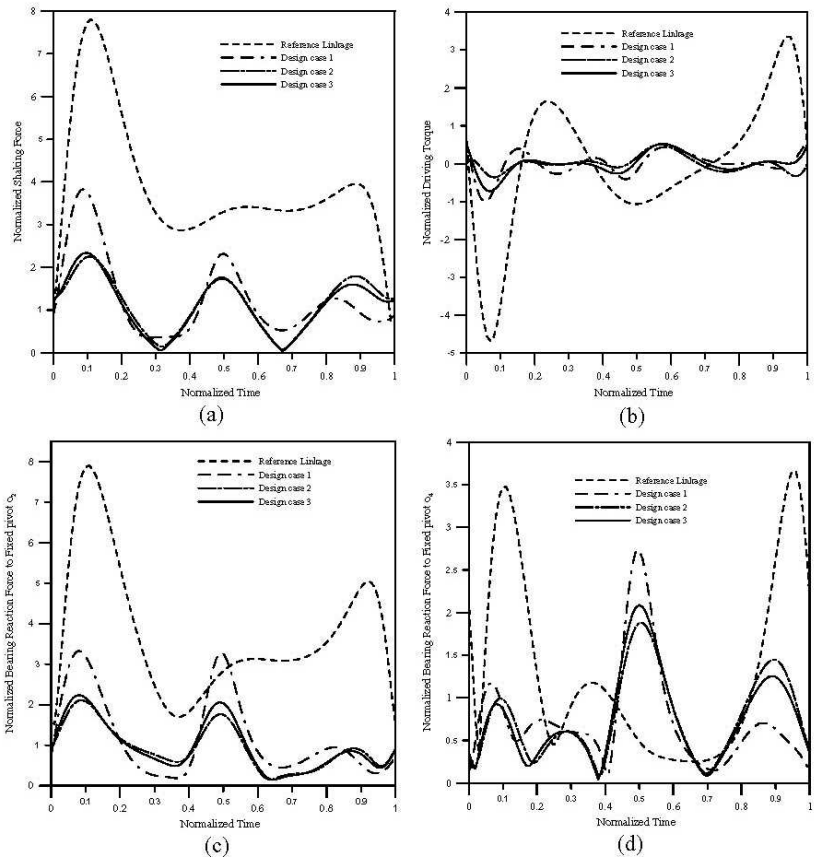

Figure 11

Dynamic balancing performance – Example 3

5. By properly designing the input speed, balancing parameters and link dimensions of a desired four-bar linkage, its kinematic design requirements and constraints including motion generation, function generation and path generation with prescribing time and the trade-off of dynamic balance can be reached simultaneously.
6. The input motion characteristics are designed with Bezier curves with undetermined control points.
7. A DSP-based controlled servomotor could generate the speed trajectory of the input link in practical applications.
8. This design approach can be extended to other types of mechanisms.

References

[1] F. L. Conte, G. R. George, R. W. Mayne and J. P. Sadler, Optimum mechanism design combining kinematic and dynamic-force considerations, *ASME Transactions, Journal of Engineering for Industry*, Series B, Vol. 95 (2) (1975), pp. 662–670.

[2] H. S. Yan and R. C. Soong (2004), An integrated design approach of four-bar linkages with variable input speed, *JSME International Journal*, Series C, Vol. 47 (1), pp. 350–362.

[3] H. S. Yan, M. H. Hsu, M. K. Fong and W. H. Hsieh, A kinematic approach for eliminating the discontinuity of motion characteristics of cam-follower systems, *Journal of Applied Mechanisms & Robotics*, Vol. 1 (2) (1994), pp. 1–6.

[4] I. S. Kochev., Full shaking moment balancing of planar linkages by a prescribed input speed fluctuation, *Mechanism and Machine Theory*, Vol. 25 (4) (1990), pp. 459–466.

[5] H. S. Yan, M. C. Tsai and M. H. Hsu, A variable-speed method for improving motion characteristics of cam-follower systems, *ASME Transactions, Journal of Mechanical Design*, Vol. 118 (1) (1996), pp. 250–258.

[6] H. S. Yan, M. C. Tsai and M. H. Hsu, An experimental study of the effects of cam speed on cam-follower systems, *Mechanism and Machine Theory*, Vol. 31 (4) (1996), pp. 397–412.

[7] H. S. Yan and W. R. Chen, On the output motion characteristics of variable input speed servo-controlled slider-crank mechanisms, *Mechanism and Machine Theory*, Vol. 35 (4) (2000), pp. 541–561.

[8] V. H. Arakelian and M. R. Smith, Complete shaking force and shaking moment balancing of linkages, *Mechanism and Machine Theory*, Vol. 34 (8) (1999), pp. 1141–1153.

[9] V. H. Arakelian and M. R. Smith, Partial shaking moment balancing of full force balanced linkages, *Mechanism and Machine Theory*, Vol. 36 (11-12) (2001), pp. 1241–1252.

[10] W. Funk, Complete balancing of the inertia input torque for planar mechanisms, *Archive of Applied Mechanics*, Vol. 63 (4-5) (1993), pp. 353–360.

[11] T. W. Lee and C. Cheng, Optimum balancing of combined shaking force, shaking moment, and torque fluctuations in high-speed linkages, *ASME Transaction, Journal of Mechanisms, Transmissions, and Automation in Design*, Vol. 106 (1984), pp. 242–251.

[12] S. J. Tricamo and G. G. Lowen, Simultaneous optimization of dynamic reactions of a four-bar linkage with prescribing maximum shaking force, *ASME Transactions, Journal of Mechanisms, Transmissions, and Automation in Design*, Vol. 105 (1983), pp. 520–525.

[13] S. T. Chiou and G. J. Bai, Optimum balancing design of four-bar linkages with adding disk counterweights, *Journal of the Chinese Society of Mechanical Engineers* (*Taiwan*), Vol. 18 (1997), pp. 43–54.

[14] N. M. Qi and E. Pennestri, Optimum balancing of four-bar linkages, *Mechanism and Machine Theory*, Vol. 26 (3) (1991), pp. 337–348.

[15] G. Guo, N. Morita and T. Torii, Optimum dynamic design of planar linkages using genetic algorithms, *JSME International Journal*, Series C, Vol. 43 (2) (2000), pp. 372–377.

[16] A. S. Hall Jr., *Notes on Mechanism Analysis*, BALT Publishers (1981), Lafayette, Indiana.

[17] C. H. Tseng, W. C. Liao and T. C. Yang, *Most Users' Manual*, Department of Mechanical Engineering, National Chiao Tung University (1994), Hsinchu, Taiwan, R.O.C.

Received July, 2006; Revised March, 2007